JOURNAL OF APPLIED CRYSTALLOGRAPHY

Volume 56 (2023)

Supporting information for article:

Multilevel Atomic Structural Model for Interstratified Opal Materials

Hsiu-Wen Wang, Katharine Page, Reinhard B. Neder, Andrew G. Stack and David L. Bish

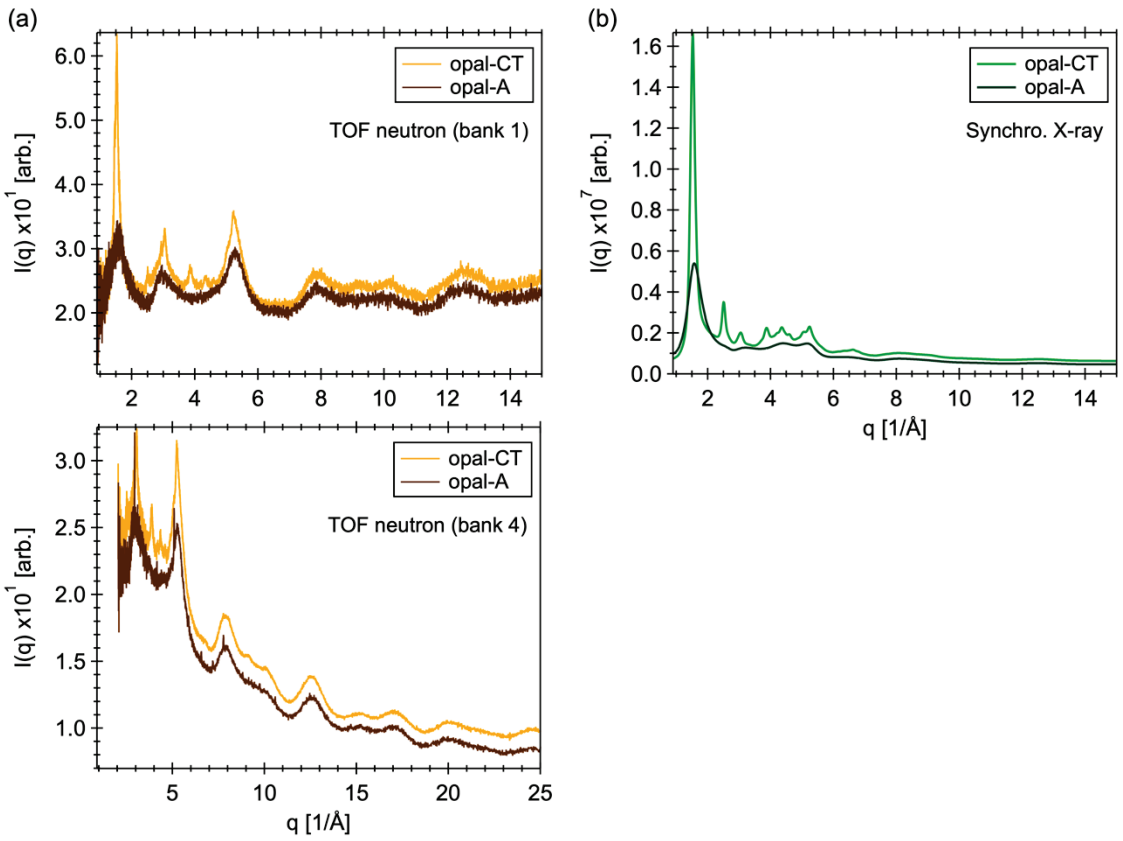

Figure S1 The reduced neutron and X-ray intensity I(q) datasets for opal-A and opal-CT samples. Note that the background and container signals are subtracted. In the neutron datasets, two selected detector banks (prior to data blending) are shown, where bank 1 is located at target angle (2θ) of 46.6° and bank 4 is at target angle (2θ) of 148.0°.

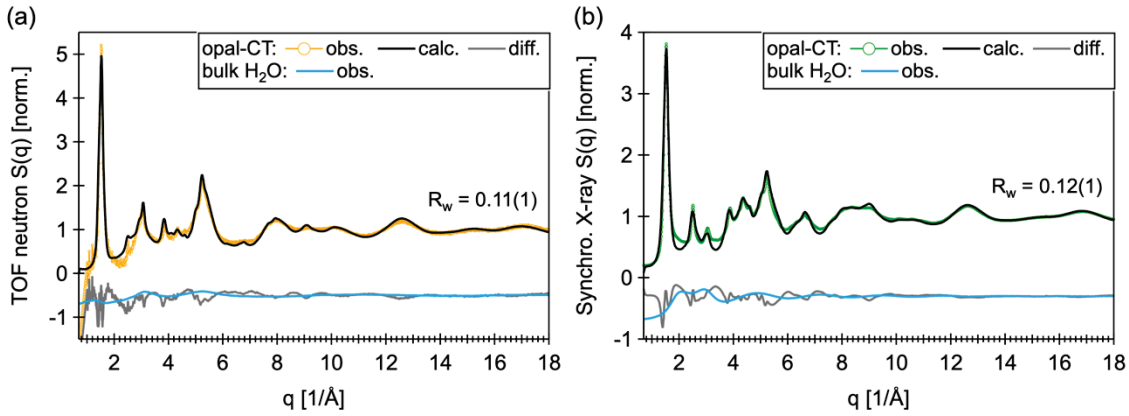

Figure S2 Model fits to (*a*) neutron and (*b*) X-ray S(q) data. Colored circles are observed data, and black curves show the calculated data using multilevel modeling approaches (population-averaged results). The differences between the observed and model data are given in gray lines shown at the bottom of each plot. Bulk water S(q) data is provided for ease of comparison. Bulk water S(q) data is adopted from Soper (2013).

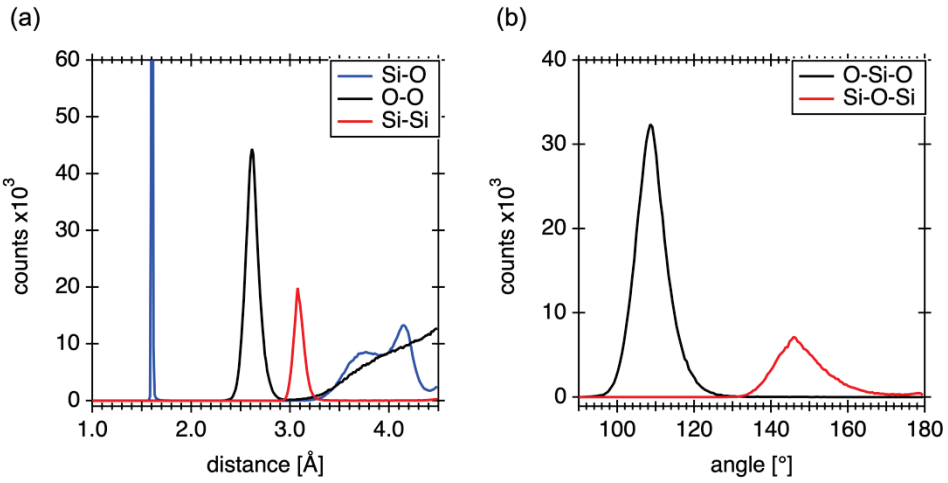

Figure S3 (*a*) Bond distances and (*b*) angle distributions for the SiO_4 intra- and inter-tetrahedral interactions.

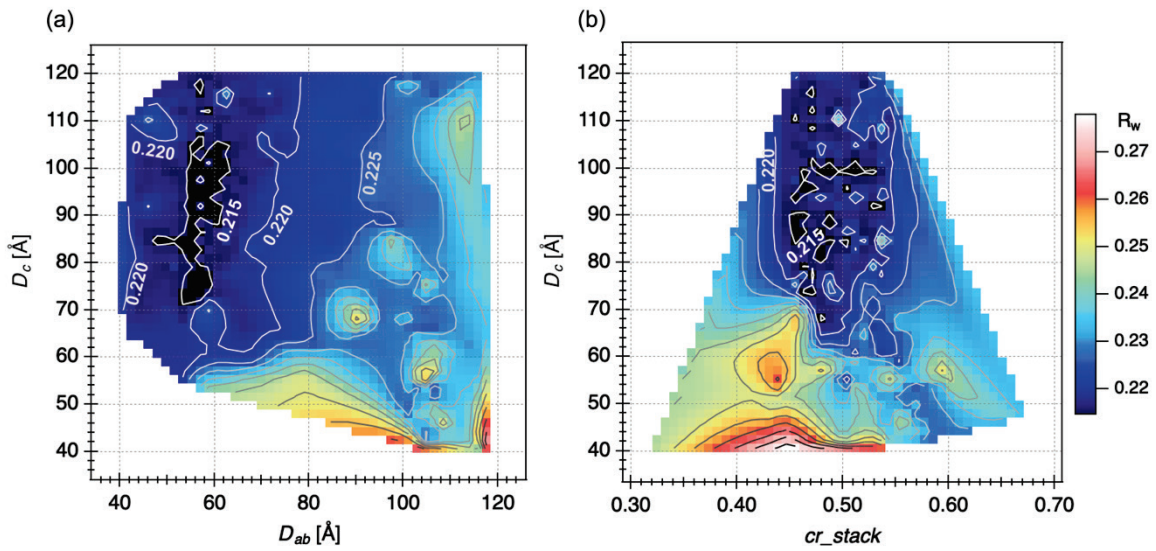

Figure S4 R_w contour maps with respect to (*a*) D_{ab} vs. D_c and (*b*) *cr_stack* vs. D_c, showing a limited range of parameter values in providing reasonable agreements.

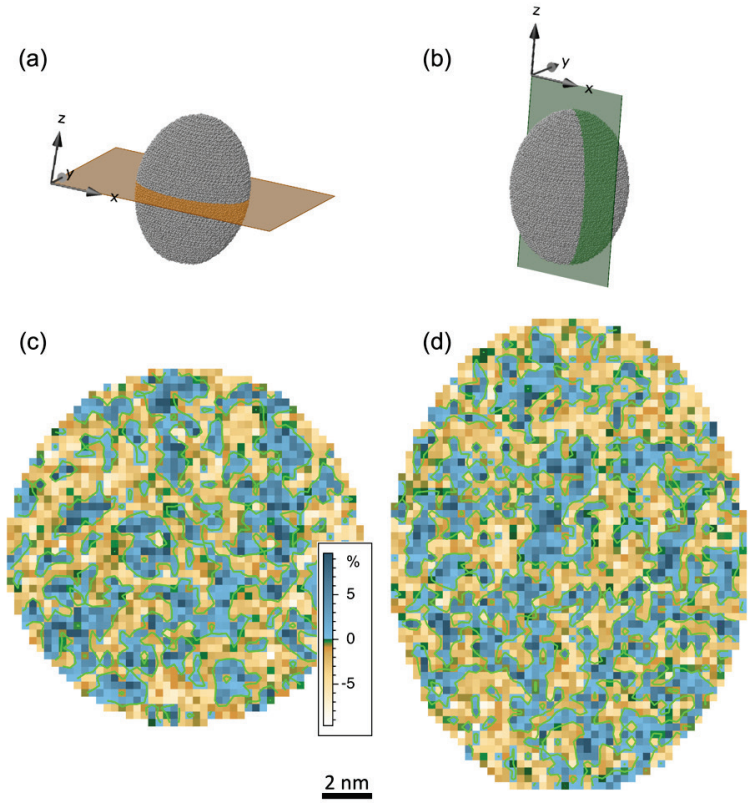

Figure S5 (*a-b*) 3D visualization of a constructed opal-CT crystallite domain (ellipsoid shape) containing ~155,000 atoms. Two different plane intercepts are displayed and were used to compute Si-O-Si bond angle strain maps shown in plots (*c*) and (*d*). The domain diameters are D_c = 200 Å and D_{ab} = 150 Å. (c-d) Si-O-Si bond angle strain analysis, showing slices through the *xy*-plane (plot (*c*)) and *xz*-plane (plot (*d*)). The strain distribution was calculated using the mean bond angle of 150°, and is visualized using a color code, scaling between ±9%.

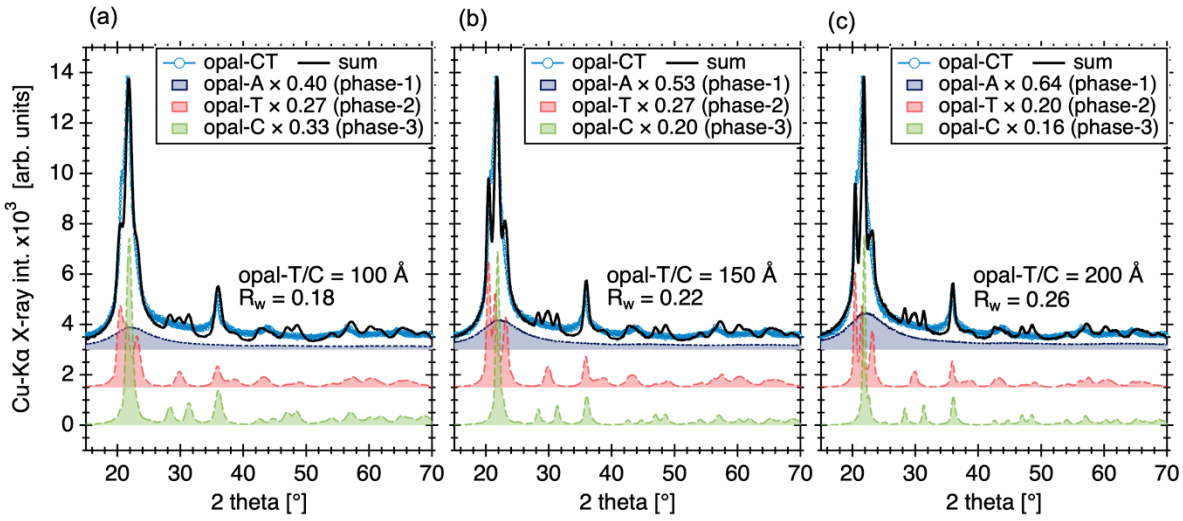

Figure S6 Measured opal-CT Cu-Kα XRD (dotted blue curve) and the comparison to modeled XRD patterns (black curve) obtained from three-phase fitting routine. The summed total (black curve) is composed of contributions of measured opal-A XRD (dark blue), and calculated opal-T (red) and opal-C (green) XRD patterns. Three different crystallite size conditions are presented, in which opal-T and opal-C XRD patterns were simulated for crystallite sizes of (*a*) 100 Å, (*b*) 150 Å and (*c*) 200 Å diameter. The number associated with each phase represents the weighting contribution (%) to the total observed intensity.

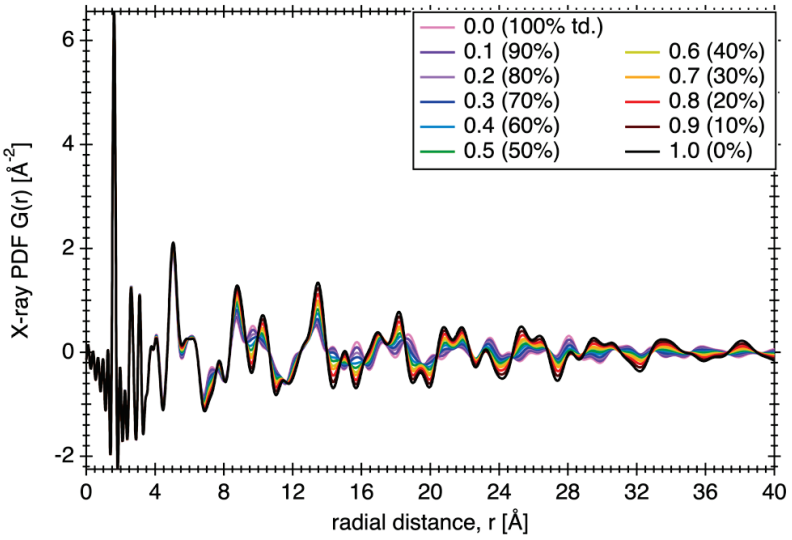

Figure S7 Montage of X-Ray PDF patterns calculated as a function of the probability that layers in an opal-CT structure will stack in cristobalitic ABC sequence. Thus, *cr_stack* = 0.0 corresponds to pure opal-T (100 % P_{td}), and *cr_stack* = 1.0 corresponds to pure opal-C (0 % P_{td}). Simulations were performed at D_{ab} = 150 Å and D_c = 200 Å (in diameter). Note that at distances < ~6 Å, all structural polymorphs have similar local pair correlations. At longer distances, the observed frequency of oscillations varies as the stacking probability is varied between 0 and 1.

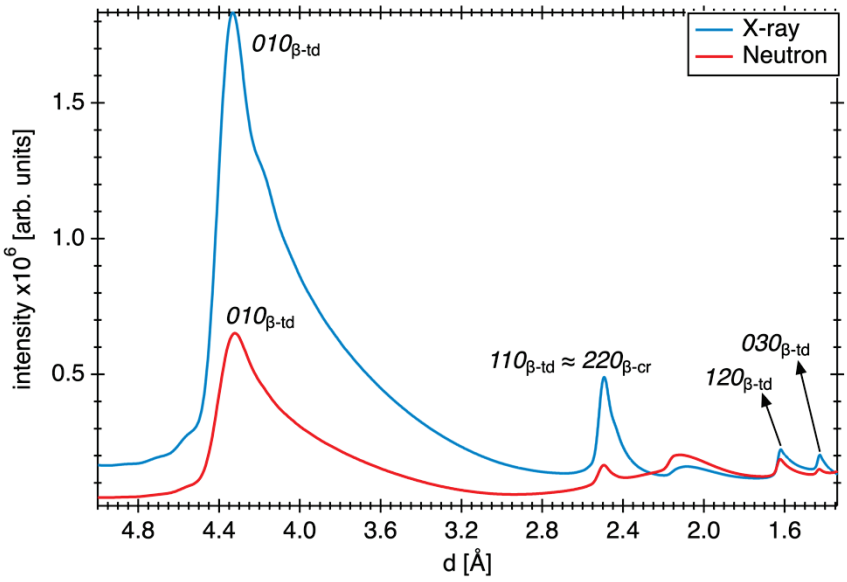

Figure S8 Calculated powder diffraction patterns of a single 2D silica layer, showing only *hk*0 reflections with strongly asymmetric line-shapes. Simulations were performed at D_{ab} = 150 Å (in diameter) with layer thickness of ~4.11Å. Wavelength λ = 1.5418 Å was used for X-ray calculation, and λ = 12.078 Å was used for neutron calculation.

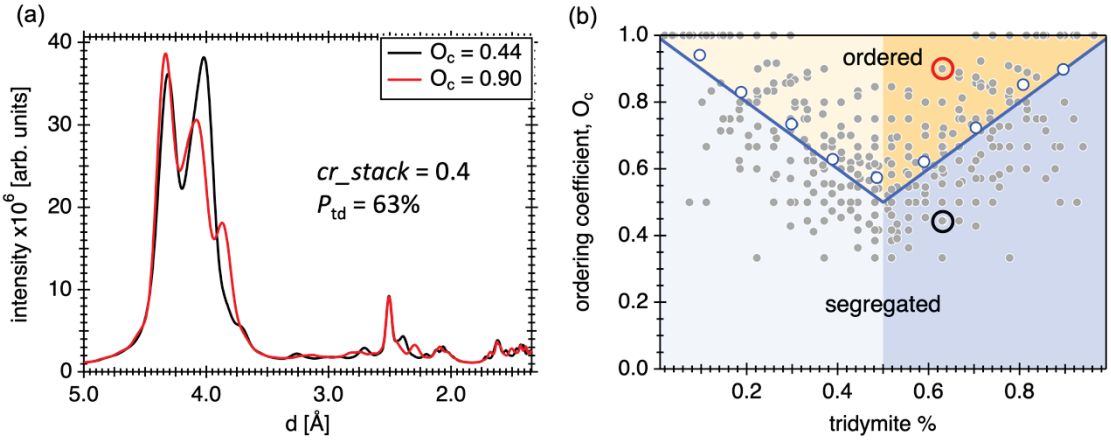

Figure S9 (*a*) Comparison of calculated X-ray powder diffraction patterns for opal-CT structures with segregated (ordering coefficient, O_c = 0.44) vs. near R1-ordered (O_c = 0.90) interstratifications. Simulations were performed at *cr_stack* = 0.4, D_{ab} = 150 Å, and D_c = 150 Å (in diameter). The resulting (averaged) probability of tridymite components P_{td} = 63%. (*b*) Demonstration of ordering state of the cristobalite-tridymite interstratification, generated via repeated simulations for a given stacking probability (*cri_stack* = 0.1-0.9) and domain sizes (D_{ab} = 150 Å and D_c = 150 Å). Individual (not averaged) interstratification configurations, as indicated by ordering coefficient (O_c), are shown as gray circles. The stacking configuration is evaluated by the relationship among O_c, P_{td}, and P_{cr} (1 − P_{td}). When $P_{td} \geq 0.5$ and $O_c > P_{td}$ or $P_{td} < 0.5$ and $O_c > P_{cr}$, an ordered interstratification is obtained (dark and light orange shadow areas). For example, O_c = 1 produces R1-ordering. When $P_{td} \geq 0.5$ and

$O_c < P_{td}$ or $P_{td} < 0.5$ and $O_c < P_{cr}$, a segregated interstratification is obtained (dark and light blue shadow areas). For example, $O_c = 0$ produces a complete segregation of cristobalite and tridymite segments. The $O_c = 0$ interstratification is difficult to achieve in our simulations because each layer only retains a memory to the first neighboring interactions. At all conditions, when $O_c = P_{td}$ a random interstratification is obtained (solid blue line with white circles). These results arise from the way in which the junction probability is defined. Other examples can be found in Guthrie *et al.* (1995), and more detailed discussions for probability and interstratification are in Reynolds (1980, 1993). In this work, for a given stacking probability, all the calculated diffraction or PDF patterns are population-averaged (white circles) and follow closely the random interstratification definition (solid blue line) shown in the plot (*b*). The two cases displayed in the plot (*a*) are marked by red and black circles in the plot (*b*).

References

Soper, A. K. (2013). *ISRN Phys. Chem.* **2013**.

Guthrie, G. D., Bish, D. L. & Reynolds, R. C. (1995). *Am. Mineral.* **80**, 869-872.

Reynolds, R. C. (1980). *Crystal Structures of Clay Minerals and their X-Ray Identification*, edited by G. W. Brindley & G. Brown, pp. 249-303. London: Mineralogical Society of Great Britain and Ireland.

Reynolds, R. C. Jr (1993). *Computer Applications to X-Ray Powder Diffraction Analysis of Clay Minerals*, edited by R. C. Reynolds Jr & R. E. Ferrell Jr, pp. 43-78. Boulder: Clay Minerals Society.